BULLETIN OF THE POLISH ACADEMY OF SCIENCES
TECHNICAL SCIENCES, Vol. 73(5), 2025, Article number: e154145
DOI: 10.24425/bpasts.2025.154145



# Analytical solution of Atangana-Baleanu fractional viscoelastic relaxation model – Laplacian approach

**Muhammad Sabeel KHAN*, Ayesha SAGHEER, and Zarafshan AZEEM**

Department of Mathematics, Capital University of Science and Technology, 44000 Islamabad, Pakistan

**Abstract.** In this contribution, a new novel approach based on the Atangana-Baleanu fractional in conjunction with the Laplacian approach is utilized to obtain an analytical solution of a fractional time relaxation viscoelastic model. The fractional time relaxation model is based on the upper convected Maxwell constitutive relaxation equation. Results for the existence and uniqueness of the solution are presented. Analytical expressions of the solutions are obtained for the underlying physical time relaxation viscoelastic model. Two test model problems with prescribed initial conditions are used to investigate the intricate behaviour of the viscoelastic two-dimensional fluid. The influence of key parameters such as relaxation time, Reynolds number and the order of the fractional derivative on fluid flow characteristics is analyzed and discussed.

**Keywords:** viscoelasticity; relaxation time; fractional derivative; analytical solution; Laplace transform.

## 1. INTRODUCTION

Time relaxation viscoelastic models have been studied in the literature for many important industrial applications. These processes range from polymeric melting processes [1, 2], pulp fibers [3] mineral processing [4], food processing [5], and biophysical processes [6,7]. Also, viscoelastic flows are seen to be generated in simple liquids by the vibration of nanostructures, see for instance [7], and references present therein.

Viscoelastic behaviour of flows has been studied in the literature so far in varying contexts. For instance, Boyang in his PhD dissertation [8] investigated the flow of polymeric viscoelastic fluid in three different geometries where it was observed that fluid relaxation influences the onset of turbulence in shear flows. For a review of the effect of viscoelastic fluid flows and their applications, the reader is referred to the work of Yuan *et al.* [9]. For a review and state-of-the-art research on viscoelastic fluids in particle focusing and related particle manipulation applications, the reader is referred to the work of Chen [6]. Swimming of ciliated cells in a viscoelastic Giesekus fluid is investigated in the work of Zhu *et al.* [10]. They observe a decay in the flow velocity of the fluid in the presence of polymeric stresses. The main characteristic of their investigation was the behaviour of the Weissenberg number on the polymeric swimmers using numerical simulation through the finite element method. Having applications in health and diseases, the review article by Sebastian and Dittrich [11], the microfluidics which are viscoelastic are used to mimic the blood flow in the human body, is highly recommended. To understand the practical application of viscoelastic fluids in porous media, the reader is referred to the work of Haward *et al.* [12]. In connection to the clinical experimentation and microfluidics to study the behaviour of neutrophil genomics and proteomics, the reader is referred to the work [13]. The flow of these complex fluids is resolved by using several numerical algorithms in the literature; in this regard, the reader is referred to a comprehensive review article in [14] on the numerical methods for viscoelastic fluid flows and flow characteristics in a two-dimensional baffled cavity, see for instance [15].

Fractional approaches to investigate such models have been applied in the literature so far and are mostly based on Caputo fractional derivatives. Fractional time analysis is constantly positioned to work on current mathematical models due to its unique potential to identify peculiar action and memory effects [16–24] which are the key components of tangled peculiarities. By working together, professionals like Caputo Riemann, Liouville, Ross and Miller, Podlubny, and others were able to resolve the mathematical basis for fragmented solicitation auxiliaries. Incomplete postmodern math conjecture was connected to real-world applications and included theories about chaos, electrodynamics, signal processing, thermodynamics, financial perspectives, and several other fields [25–29].

Recently, researchers have given more attention to fractional derivatives, their applications and analysis [30]. Fractional derivative on the multilayered Navier-Stokes condition to analyze the nature of the flow, see for instance [31]. A study presents a numerical method for solving nonhomogeneous two-dimensional fractional integro-differential equations using the modified Atangana-Baleanu fractional derivative, employing operational matrices to convert the problem into an algebraic system, with examples demonstrating the method efficiency [32]. Another study presented a numerical method for solving one- and two-dimensional Burgers' equations involving time fractional Atangana-Baleanu Caputo derivatives, using Haar wavelet approximations and a quadrature rule for the fractional derivative, with the results demonstrating its effectiveness, better performance than existing methods, and a convergence rate

*e-mail: muhammad.sabeel@cust.edu.pk

Manuscript submitted 2024-11-22, revised 2025-02-17, initially accepted for publication 2025-02-27, published in July 2025.

of order two [33]. There are many other such studies in the literature that highlight the importance of fractional derivatives, especially Atangana-Baleanu fractional derivative, in solving systems of PDEs. Interested readers can check out [34–36].

This study uses a novel approach combining the Atangana-Baleanu fractional and Laplacian approaches to solving a fractional time relaxation viscoelastic model. Atangana-Baleanu fractional derivative was chosen out of all the different fractional derivatives because it has been proven that Atangana-Baleanu derivative provides more accurate results compared to the standard derivative with an exponential kernel, offering a generalized approach for modelling. In a study conducted in 2018 [37], the real-world applications of Atangana-Baleanu derivative were discussed, in specific, investigating various modelling problems, including Newton's law of cooling, population growth, logistic equation, and the blood alcohol model. And the analytical solutions are derived through the Laplace transform, with results visualized through simulations for different fractional orders, which offer results with uncanny accuracy.

The model used for this study is based on the upper convected Maxwell constitutive relaxation equation. The study investigates viscoelastic two-dimensional fluid behaviour, analyzing key parameters and their impact on fluid flow characteristics. The rest of the article is organized as follows: in Section 2, the fractional time relaxation viscoelastic model is presented. The model is nondimensionalized and two test cases are prescribed. In Section 3, some mathematical preliminaries are stated. In Section 4, theoretical results for the existence and uniqueness of the solution are shown. In Section 5, the presented model problem is solved for the two test cases and analytical expressions of the solutions are obtained in each case. Moreover, results are presented graphically for varying relaxation time, Reynolds number and the order of the fractional derivative and solution characteristics are discussed. Finally, conclusions are drawn in Section 6.

## 2. FRACTIONAL TIME RELAXATION VISCOELASTIC MODEL

One of the widely appreciated models to describe viscoelastic fluids is the upper convected Maxwell (UCM) model that incorporates viscosity and relaxation time with the following constitutive equation:

$$\lambda \nabla_\tau + \boldsymbol{\tau} = -2\eta\, \boldsymbol{d}(\boldsymbol{v}), \tag{1}$$

where $\lambda$ and $\eta$ are the fluid characteristic relaxation time and the fluid viscosity, respectively. The deformation strain tensor $\boldsymbol{d}(\boldsymbol{v})$ in (1) is defined as

$$\boldsymbol{d}(\boldsymbol{v}) = \frac{1}{2}\left(\nabla \boldsymbol{v} + (\nabla \boldsymbol{v})^T\right). \tag{2}$$

In (1), $\nabla_\tau$ is the upper convected derivative defined as

$$\nabla_\tau = \frac{\partial \boldsymbol{\tau}}{\partial t} + \boldsymbol{v}\cdot\nabla\boldsymbol{\tau} - \nabla\boldsymbol{v}\cdot\boldsymbol{\tau} - \boldsymbol{\tau}\cdot(\nabla\boldsymbol{v})^T. \tag{3}$$

Here, $\lambda$ and $\eta$ are assumed to be constant, whereas in general, they may depend upon the local shear rate, pressure, and temperature. The dynamics of viscoelastic fractional time relaxation flow are governed by the following partial differential equation

$$\rho\left(D_t^\alpha(\boldsymbol{v}) + \boldsymbol{v}\cdot\nabla\boldsymbol{v}\right) + \nabla p + \nabla\cdot\boldsymbol{\tau} = \boldsymbol{b}, \tag{4}$$

together with the mass conservation within the flow domain

$$\nabla\cdot\boldsymbol{v} = 0. \tag{5}$$

Consider a two-dimensional unsteady incompressible viscoelastic flow having velocity field $\boldsymbol{v} = (u, v)$ in the coordinates $(x, y)$. In the absence of body forces $\boldsymbol{b}$, the continuity and momentum equations (5) and (4), respectively reads in the component form as

$$\frac{\partial u}{\partial x} + \frac{\partial v}{\partial y} = 0, \tag{6}$$

$$D_t^\alpha(u) + u\frac{\partial u}{\partial x} + v\frac{\partial u}{\partial y} + \lambda\left(u^2\frac{\partial^2 u}{\partial x^2} + v^2\frac{\partial^2 u}{\partial y^2} + 2uv\frac{\partial^2 u}{\partial x\partial y}\right) = -\frac{1}{\rho}\frac{\partial p}{\partial x} + \eta\left(\frac{\partial^2 u}{\partial x^2} + \frac{\partial^2 u}{\partial y^2}\right), \tag{7}$$

and

$$D_t^\alpha(v) + u\frac{\partial v}{\partial x} + v\frac{\partial v}{\partial y} + \lambda\left(u^2\frac{\partial^2 v}{\partial x^2} + v^2\frac{\partial^2 v}{\partial y^2} + 2uv\frac{\partial^2 v}{\partial x\partial y}\right) = -\frac{1}{\rho}\frac{\partial p}{\partial y} + \eta\left(\frac{\partial^2 v}{\partial x^2} + \frac{\partial^2 v}{\partial y^2}\right). \tag{8}$$

To aid analysis and calculation, the following variables have been introduced to equations (6)-(8) as dimensionless.

$$\begin{aligned} U &= \frac{u}{u_0}, \quad V = \frac{v}{u_0}, \quad T = \frac{tL}{u_0}, \\ X &= \frac{x}{L}, \quad y = \frac{y}{L}, \quad P = \frac{p}{\rho u_0^2}, \end{aligned} \tag{9}$$

where $L$ is the characteristic length of the flow domain considered and $u_0$ is the assumed ambient velocity. Now, using (9) in equations (6)–(8) leads to the following nondimensional set of PDEs. Detailed calculations for the following results can be observed in the Appendix section.

$$\frac{\partial U}{\partial X} + \frac{\partial V}{\partial Y} = 0, \tag{10}$$

$$D_T^\alpha(U) + U\frac{\partial U}{\partial X} + V\frac{\partial U}{\partial Y} + R_f\left(U^2\frac{\partial^2 U}{\partial X^2} + V^2\frac{\partial^2 U}{\partial Y^2} + 2UV\frac{\partial^2 U}{\partial X\partial Y}\right) = -\frac{\partial P}{\partial X} + \frac{1}{R_e}\left(\frac{\partial^2 U}{\partial X^2} + \frac{\partial^2 U}{\partial Y^2}\right), \tag{11}$$

and

$$D_T^{\alpha}(V)+U\frac{\partial V}{\partial X}+V\frac{\partial V}{\partial Y}+R_f\left(U^2\frac{\partial^2 V}{\partial X^2}+V^2\frac{\partial^2 V}{\partial Y^2}+2UV\frac{\partial^2 V}{\partial X\partial Y}\right)$$
$$=-\frac{\partial P}{\partial Y}+\frac{1}{R_e}\left(\frac{\partial^2 V}{\partial X^2}+\frac{\partial^2 V}{\partial Y^2}\right). \quad (12)$$

In (11) and (12), the dimensionless parameters $R_e$ and $R_f$ represent Reynolds number, and fluid relaxation time, respectively, and are defined by

$$R_f=\frac{\lambda u_0}{L}, \quad \text{and} \quad R_e=\frac{\rho L u_0}{\mu}. \quad (13)$$

The aim here is to seek the solution for the above set of PDEs in (6)–(8) with the following two sets of initial conditions.

- Case 1: $U(X,Y,0)=e^X, \quad V(X,Y,0)=e^Y$.
- Case 2: $U(X,Y,0)=XY^2-XY, \quad V(X,Y,0)=X^2Y-XY$.

The analytical solution is sought by the application of the Laplace transform together with the Atangana-Baleanu fractional derivative. In the next section, we present the existence and uniqueness results.

## 3. MATHEMATICAL PRELIMINARIES

To state the results and construction of their proofs let us define the following mathematical preliminaries.

### 3.1. Definitions

#### 3.1.1. ]

Atangana-Baleanu fractional derivative [30]

Let $h\in H(0,1)$ and $0<n<1$, the Atangana-Baleanu fractional derivative in the Caputo sense is defined as

$$T_n(h)(x)=\frac{B(n)}{1-n}\int_0^x E_n\left[\frac{-n}{1-n}(x-s)^n\right]h'(s)\,\mathrm{d}s. \quad (14)$$

#### 3.1.2. ]

Atangana-Baleanu integral operator [30]

The Atangana-Baleanu integral operator of function $f$ and order $n$ is given as

$${}_a^{AB}I_0^n f(t)=\frac{1-n}{B(n)}f(t)+\frac{n}{B(\alpha)\Gamma(n)}\int_a^t f(y)(t-y)^{n-1}\,\mathrm{d}y.$$

#### 3.1.3. ]

Atangana-Baleanu integral operator (in Caputo-sense) [30]

The Atangana-Baleanu integral operator (in the Caputo-sense) of function $f$ and order $n$ is defined as

$${}_a^{ABC}I_t^n f(t)=\frac{1-n}{B(n)}f(t)+\frac{n}{B(n)\Gamma(n)}\int_0^t f(y)(t-y)^{n-1}\,\mathrm{d}y.$$

#### 3.1.4. Laplace change of Atangana-Baleanu derivative

The Laplace change of the Atangana-Baleanu derivative [38] of order $\tau$ is given by

$$\mathscr{L}\left\{{}^{ABC}D^{\tau}f(t)\right\}=\frac{M(\tau)}{1-\tau}\cdot\frac{p^{\tau}\mathscr{L}\{f(t)\}-p^{\tau-1}f(0)}{p^{\tau}+\frac{\tau}{1-\tau}}.$$

## 4. EXISTENCE AND UNIQUENESS RESULTS

The relaxation time model in (11) and (12) is requested with the application of the Atangana-Baleanu fractional time derivative in the Caputo sense as

$${}^{ABC}D_T^n(U)=-U\frac{\partial U}{\partial X}-V\frac{\partial U}{\partial Y}-R_f\left(U^2\frac{\partial^2 U}{\partial X^2}\right.$$
$$\left.+V^2\frac{\partial^2 U}{\partial Y^2}+2UV\frac{\partial^2 U}{\partial X\partial Y}\right)-\frac{\partial P}{\partial X}+\frac{1}{R_e}\left(\frac{\partial^2 U}{\partial X^2}+\frac{\partial^2 U}{\partial Y^2}\right),$$
$${}^{ABC}D_T^n(V)=-U\frac{\partial V}{\partial X}-V\frac{\partial V}{\partial Y}-R_f\left(U^2\frac{\partial^2 V}{\partial X^2}+V^2\frac{\partial^2 V}{\partial Y^2}\right.$$
$$\left.2UV\frac{\partial^2 V}{\partial X\partial Y}\right)-\frac{\partial P}{\partial Y}+\frac{1}{R_e}\left(\frac{\partial^2 V}{\partial X^2}+\frac{\partial^2 V}{\partial Y^2}\right). \quad (15)$$

With a given set of initial conditions this set of PDEs in (15) admit solution which is guaranteed by the following result.

**Theorem 1.** Let $\mathbf{U}=(U,V)$. Suppose $\mathbf{f}(X,t,\mathbf{U},\mathbf{U}_X,\mathbf{U}_Y,\mathbf{U}_{XX},\mathbf{U}_{XY},\mathbf{U}_{YY})$ satisfies the Lipschitz condition in each of its arguments with the Lipschitz constant i.e.,

$$L=K+\sum_{i=1}^{5}K_i\delta_i.$$

Further, assume that $\exists$ scalars $\delta_j\in R^+$ such that

$$\left\|\mathbf{U}_{i,m}-\bar{\mathbf{U}}_{i,m-1}\right\|\le\delta_j\left\|\mathbf{U}_m-\bar{\mathbf{U}}_{m-1}\right\|,$$

where $i$ takes values from the set $\{X,Y,XX,YY,XY\}$ and $m\in Z^+$, then the solution to the system in (15) exists if

$$\frac{1-n}{B(n)}+\frac{t_{\max}^n}{B(n)\Gamma(n)}<1.$$

**Proof.** Applying the fundamental premise of fractional calculus,we can write

$$\mathbf{U}(X,t)-\mathbf{U}(X,0)=\left(\frac{1-n}{B(n)}\right)\mathbf{f}(X,t,\mathbf{U},\mathbf{U}_X,\mathbf{U}_Y,\mathbf{U}_{XX},\mathbf{U}_{XY},\mathbf{U}_{YY})$$
$$+\frac{n}{B(n)\Gamma(n)}\int_0^t(t-\xi)^{n-1}$$
$$\cdot\mathbf{f}(X,t,\mathbf{U},\mathbf{U}_X,\mathbf{U}_Y,\mathbf{U}_{XX},\mathbf{U}_{XY},\mathbf{U}_{YY})\,\mathrm{d}\xi, \quad (16)$$

or,

$$\mathbf{U}(\boldsymbol{X},t)=\mathbf{U}_0+\frac{1-n}{B(n)}\mathbf{f}\big(\boldsymbol{X},t,\mathbf{U},\mathbf{U}_X,\mathbf{U}_Y,\mathbf{U}_{XX},\mathbf{U}_{XY},\mathbf{U}_{YY}\big)+\frac{n}{B(n)\Gamma(n)}\int_0^t(t-\xi)^{n-1}\mathbf{f}(\boldsymbol{X},t,\mathbf{U},\mathbf{U}_X,\mathbf{U}_Y,\mathbf{U}_{XX},\mathbf{U}_{XY},\mathbf{U}_{YY})\,\mathrm{d}\xi. \quad (17)$$

Assuming that $\mathbf{U}$ is a solution of (15) at the $m^{th}$ time step, an explicit relation can be obtained as

$$\mathbf{U}_m(\boldsymbol{X},t)=\mathbf{U}_0+\frac{1-n}{B(n)}\mathbf{f}\big(\boldsymbol{X},t,\mathbf{U}_{m-1},\mathbf{U}_{X,m-1},\mathbf{U}_{Y,m-1},\mathbf{U}_{XX,m-1},\mathbf{U}_{XY,m-1},\mathbf{U}_{YY,m-1}\big)+\frac{n}{B(n)\Gamma(n)}\int_0^t(t-\xi)^{n-1}\mathbf{f}\big(\boldsymbol{X},t,\mathbf{U}_{m-1},\mathbf{U}_{X,m-1},\mathbf{U}_{Y,m-1},\mathbf{U}_{XX,m-1},\mathbf{U}_{XY,m-1},\mathbf{U}_{YY,m-1}\big)\,\mathrm{d}\xi. \quad (18)$$

Let $\beta_m=\mathbf{U}_m-\mathbf{U}_{m-1}$, then from (18) we can write

$$\beta_m=\frac{1-n}{B(n)}\Big[\mathbf{f}\big(\boldsymbol{X},t,\mathbf{U}_{m-1},\mathbf{U}_{X,m-1},\mathbf{U}_{Y,m-1},\mathbf{U}_{XX,m-1},\mathbf{U}_{XY,m-1},\mathbf{U}_{YY,m-1}\big)-\mathbf{f}\big(\boldsymbol{X},t,\mathbf{U}_{m-2},\mathbf{U}_{X,m-2},\mathbf{U}_{Y,m-2},\mathbf{U}_{XX,m-2},\mathbf{U}_{XY,m-2},\mathbf{U}_{YY,m-2}\big)\Big]+\frac{n}{B(n)\Gamma(n)}\int_0^t(t-\xi)^{n-1}\Big[\mathbf{f}\big(\boldsymbol{X},t,\mathbf{U}_{m-1},\mathbf{U}_{X,m-1},\mathbf{U}_{Y,m-1},\mathbf{U}_{XX,m-1},\mathbf{U}_{XY,m-1},\mathbf{U}_{YY,m-1}\big)-\mathbf{f}\big(\boldsymbol{X},t,\mathbf{U}_{m-2},\mathbf{U}_{X,m-2},\mathbf{U}_{Y,m-2},\mathbf{U}_{XX,m-2},\mathbf{U}_{XY,m-2},\mathbf{U}_{YY,m-2}\big)\Big]\mathrm{d}\xi. \quad (19)$$

Let us use the following notations for convenience

$$f_{m-1}=\mathbf{f}\big(\boldsymbol{X},t,\mathbf{U}_{m-1},\mathbf{U}_{X,m-1},\mathbf{U}_{Y,m-1},\mathbf{U}_{XX,m-1},\mathbf{U}_{XY,m-1},\mathbf{U}_{YY,m-1}\big),$$
$$f_{m-2}=\mathbf{f}\big(\boldsymbol{X},t,\mathbf{U}_{m-2},\mathbf{U}_{X,m-2},\mathbf{U}_{Y,m-2},\mathbf{U}_{XX,m-2},\mathbf{U}_{XY,m-2},\mathbf{U}_{YY,m-2}\big),$$

then taking norm on both the sides of (19) and using triangular inequality we get

$$\|\beta_m\|\le\frac{1-n}{B(n)}\|f_{m-1}-f_{m-2}\|+\frac{n}{B(n)\Gamma(n)}\int_0^t(t-\xi)^{n-1}\|f_{m-1}-f_{m-2}\,\mathrm{d}\xi\|. \quad (20)$$

Now, since $f$ is Lipschitz in its each argument, therefore

$$\beta_m\le\frac{1-n}{B(n)}\Big[K\mathbf{U}_{m-1}-\mathbf{U}_{m-2}+K_1\mathbf{U}_{X,m-1}-\mathbf{U}_{X,m-2}+K_2\mathbf{U}_{Y,m-1}-\mathbf{U}_{Y,m-2}+K_3\mathbf{U}_{XX,m-1}-\mathbf{U}_{XX,m-2}+K_4\mathbf{U}_{XY,m-1}-\mathbf{U}_{XY,m-2}+K_5\mathbf{U}_{YY,m-1}-\mathbf{U}_{YY,m-2}\Big]+\frac{n}{B(n)\Gamma(n)}\int_0^t(t-\xi)^{n-1}\mathrm{d}\xi\Big[K\mathbf{U}_{m-1}-\mathbf{U}_{m-2}+K_1\mathbf{U}_{X,m-1}-\mathbf{U}_{X,m-2}+K_2\mathbf{U}_{Y,m-1}-\mathbf{U}_{Y,m-2}+K_3\mathbf{U}_{XX,m-1}-\mathbf{U}_{XX,m-2}+K_4\mathbf{U}_{XY,m-1}-\mathbf{U}_{XY,m-2}+K_5\mathbf{U}_{YY,m-1}-\mathbf{U}_{YY,m-2}\Big], \quad (21)$$

this implies

$$\|\beta_m\|\le\Big[K\|\mathbf{U}_{m-1}-\mathbf{U}_{m-2}\|+K_1\|\mathbf{U}_{X,m-1}-\mathbf{U}_{X,m-2}\|+K_2\|\mathbf{U}_{Y,m-1}-\mathbf{U}_{Y,m-2}\|+K_3\|\mathbf{U}_{XX,m-1}-\mathbf{U}_{XX,m-2}\|+K_4\|\mathbf{U}_{XY,m-1}-\mathbf{U}_{XY,m-2}\|+K_5\|\mathbf{U}_{YY,m-1}-\mathbf{U}_{YY,m-2}\|\Big]\left[\frac{1-n}{B(n)}+\frac{n}{B(n)\Gamma(n)}\int_0^t(t-\xi)^{n-1}\mathrm{d}\xi\right], \quad (22)$$

$$\|\beta_m\|<\Big[K\|\beta_{m-1}\|+K_1\delta_1\|\beta_{m-1}\|+K_2\delta_2\|\beta_{m-1}\|+K_3\delta_3\|\beta_{m-1}\|+K_4\delta_4\|\beta_{m-1}\|+K_5\delta_5\|\beta_{m-1}\|\Big]\cdot\left[\frac{1-n}{B(n)}+\frac{n}{B(n)\Gamma(n)}\int_0^t(t-\xi)^{n-1}\mathrm{d}\xi\right], \quad (23)$$

$$\|\beta_m\|<\|\beta_{m-1}\|\Big[K+K_1\delta_1+K_2\delta_2+K_3\delta_3+K_4\delta_4+K_5\delta_5\Big]\cdot\left[\frac{1-n}{B(n)}+\frac{n}{B(n)\Gamma(n)}\int_0^t(t-\xi)^{n-1}\mathrm{d}\xi\right]. \quad (24)$$

Leaving $K+\sum_{i=1}^{5}K_i\delta_i=L<1$, it can be stated that

$$\|\beta_m\|<L\|\beta_{m-1}\|\left[\frac{1-n}{B(n)}+\frac{n}{B(n)\Gamma(n)}\int_0^t(t-\xi)^{n-1}\mathrm{d}\xi\right].$$

It is now easy to see that

$$\|\beta_m\|\le\|\beta_0\|L^m\left[\frac{1-n}{B(n)}+\frac{n}{B(n)\Gamma(n)}\int_0^t(t-\xi)\,\mathrm{d}\xi\right]^m,$$

further, $t_{\max}$ can be chosen such that

$$\|\beta_m\|<\|\beta_0\|L^m\left[\frac{1-n}{B(n)}+\frac{t_{\max}^n}{B(n)\Gamma(n)}\right]^m.$$

Therefore, the solution to the system in (15) exists if $t_{\max}$ is such that

$$\left[\frac{1-n}{B(n)}+\frac{t_{\max}^{n}}{B(n)\Gamma(n)}\right]<1.$$

### 4.1. Uniqueness of the solution:

**Corollary 1.** The solution of (15) is unique.

**Proof.** Assume that the system in (15) has two distinct solutions i.e., $\mathbf{U}_{m,1}(\boldsymbol{X},t)$ and $\mathbf{U}_{m,2}(\boldsymbol{X},t)$. Let

$$\chi=\left(\mathbf{U},\mathbf{U}_X,\mathbf{U}_Y,\mathbf{U}_{XX},\mathbf{U}_{XY},\mathbf{U}_{YY}\right).$$

Denote

$$\mathbf{f}_{\chi_i}=\mathbf{f}(\boldsymbol{X},t,\chi_i),\quad \text{for}\quad i=1,2.$$

Consider

$$\mathbf{U}_{m,1}(\boldsymbol{X},t)-\mathbf{U}_{m,2}(\mathbf{X},t)=\frac{1-n}{B(n)}\left(\mathbf{f}_{\chi_1}-\mathbf{f}_{\chi_2}\right)+\frac{n}{B(n)\Gamma(n)}\int_0^t(t-\xi)^{n-1}\left(\mathbf{f}_{\chi_1}-\mathbf{f}_{\chi_2}\right)\mathrm{d}\xi. \quad (25)$$

Taking norm on both sides, we obtain

$$\left\|\mathbf{U}_{m,1}(\boldsymbol{X},t)-\mathbf{U}_{m,2}(\boldsymbol{X},t)\right\|=\left\|\frac{1-n}{B(n)}\left(\mathbf{f}_{\chi_1}-\mathbf{f}_{\chi_2}\right)+\frac{n}{B(n)\Gamma(n)}\int_0^t(t-\xi)^{n-1}\left(\mathbf{f}_{\chi_1}-\mathbf{f}_{\chi_2}\right)\mathrm{d}\xi\right\|, \quad (26)$$

$$\Longrightarrow\left\|\mathbf{U}_{m,1}(\boldsymbol{X},t)-\mathbf{U}_{m,2}(\boldsymbol{X},t)\right\|\leq\frac{1-n}{B(n)}\left\|\mathbf{f}_{\chi_1}-\mathbf{f}_{\chi_2}\right\|+\frac{n}{B(n)\Gamma(n)}\int_0^t(t-\xi)^{n-1}\left\|\mathbf{f}_{\chi_1}-\mathbf{f}_{\chi_2}\right\|\mathrm{d}\xi. \quad (27)$$

Since $f$ is Lipschitz, therefore

$$\left\|\mathbf{U}_{m,1}(\boldsymbol{X},t)-\mathbf{U}_{m,2}(\boldsymbol{X},t)\right\|<\left\|\mathbf{U}_0\right\|L^m\left[\frac{1-n}{B(n)}+\frac{n}{B(n)\Gamma(n)}\int_0^t(t-\xi)\,\mathrm{d}\xi\right]^m. \quad (28)$$

Applying limit

$$\lim_{m\to\infty}\left\|\mathbf{U}_{m,1}(\boldsymbol{X},t)-\mathbf{U}_{m,2}(\boldsymbol{X},t)\right|<\lim_{m\to\infty}\left\|\mathbf{U}_0\right\|L^m\left[\frac{1-n}{B(n)}+\frac{n}{B(n)\Gamma(n)}\int_0^t(t-\xi)\,\mathrm{d}\xi\right]^m. \quad (29)$$

As $L<1$, therefore

$$\lim_{m\to\infty}\left\|\mathbf{U}_{m,1}-\mathbf{U}_{m,2}\right\|\to 0$$

this implies

$$\mathbf{U}_{m,1}=\mathbf{U}_{m,2}.$$

## 5. SOLUTION BY LAPLACE TRANSFORM WITH ATANGANA-BALEANU DERIVATIVE

The system in (15) is now solved by the application of Laplace transform with the Atangana-Baleanu derivative approach as explained in the flowchart in Fig. 1. The system of PDEs is re-expressed as

$${}^{ABC}D_t^n(U)=-U\frac{\partial U}{\partial X}-V\frac{\partial U}{\partial Y}-R_f\left(U^2\frac{\partial^2U}{\partial X^2}+V^2\frac{\partial^2U}{\partial Y^2}+2UV\frac{\partial^2U}{\partial X\partial Y}\right)-\frac{\partial P}{\partial X}+\frac{1}{R_e}\left(\frac{\partial^2U}{\partial X^2}+\frac{\partial^2U}{\partial Y^2}\right), \quad (30)$$

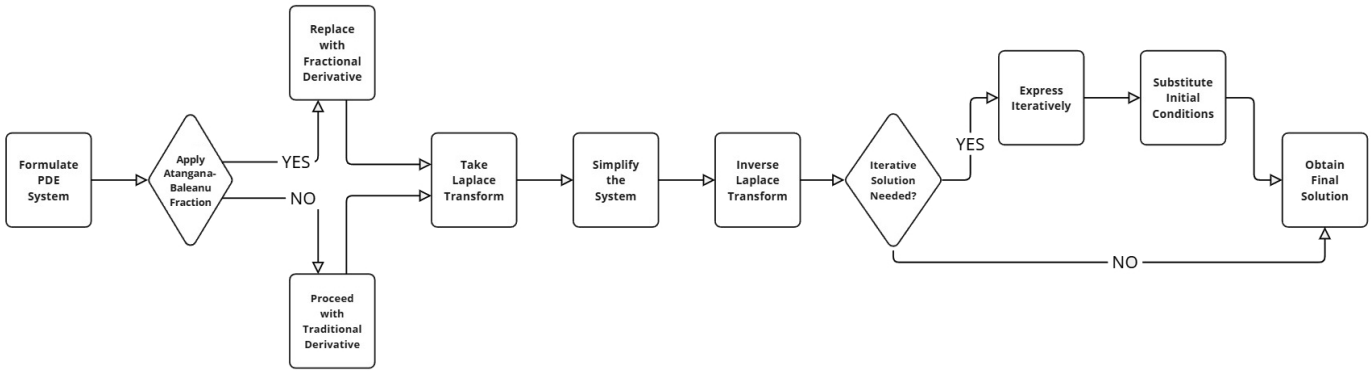


**Fig. 1.** Flowchart outlining the steps for solving a system of PDEs using the Laplace transform and iterative approach with the Atangana-Baleanu fractional derivative

and

$$
\begin{aligned}
{}^{ABC}D_t^n(V) = &-U\frac{\partial V}{\partial X} - V\frac{\partial V}{\partial Y} \\
&- R_f\left(U^2\frac{\partial^2 V}{\partial X^2} + V^2\frac{\partial^2 V}{\partial Y^2} + 2UV\frac{\partial^2 V}{\partial X \partial Y}\right) \\
&- \frac{\partial P}{\partial Y} + \frac{1}{R_e}\left(\frac{\partial^2 V}{\partial X^2} + \frac{\partial^2 V}{\partial Y^2}\right). \quad (31)
\end{aligned}
$$

Here, $n$ is the order of derivative in time $t$. Since we know that

$$
\mathscr{L}\left\{{}^{ABC}D^{\tau} f(t)\right\} = \frac{M(\tau)}{1-\tau}\cdot\frac{p^{\tau}\mathscr{L}\{f(t)\} - p^{\tau-1}f(0)}{p^{\tau} + \frac{\tau}{1-\tau}}. \quad (32)
$$

Take the Laplace transform of both sides in the first equation of (30)

$$
\begin{aligned}
\mathscr{L}\left\{{}^{ABC}D_t^n(U)\right\} = \mathscr{L}\Bigg\{&-U\frac{\partial U}{\partial X} \\
&- V\frac{\partial U}{\partial Y} - R_f\left(U^2\frac{\partial^2 U}{\partial X^2} + V^2\frac{\partial^2 U}{\partial Y^2} + 2UV\frac{\partial^2 U}{\partial X \partial Y}\right) \\
&- \frac{\partial P}{\partial X} + \frac{1}{R_e}\left(\frac{\partial^2 U}{\partial X^2} + \frac{\partial^2 U}{\partial Y^2}\right)\Bigg\}. \quad (33)
\end{aligned}
$$

Using (32) in (33) $\Longrightarrow$

$$
\begin{aligned}
\frac{M(n)}{1-n}\cdot\frac{p^n\mathscr{L}\{U(t)\} - p^{n-1}U(0)}{p^n + \frac{n}{1-n}} = \\
\mathscr{L}\Bigg\{-U\frac{\partial U}{\partial X} - V\frac{\partial U}{\partial Y} - R_f\left(U^2\frac{\partial^2 U}{\partial X^2} + V^2\frac{\partial^2 U}{\partial Y^2}\right. \\
\left. + 2UV\frac{\partial^2 U}{\partial X \partial Y}\right) - \frac{\partial P}{\partial X} + \frac{1}{R_e}\left(\frac{\partial^2 U}{\partial X^2} + \frac{\partial^2 U}{\partial Y^2}\right)\Bigg\}, \quad (34)
\end{aligned}
$$

$\Longrightarrow$

$$
\begin{aligned}
\frac{p^n\mathscr{L}\{U(t)\} - p^{n-1}U(0)}{p^n + \frac{n}{1-n}} = \frac{1-n}{M(n)}\mathscr{L}\Bigg\{&-U\frac{\partial U}{\partial X} - V\frac{\partial U}{\partial Y} \\
&- R_f\left(U^2\frac{\partial^2 U}{\partial X^2} + V^2\frac{\partial^2 U}{\partial Y^2} + 2UV\frac{\partial^2 U}{\partial X \partial Y}\right) \\
&- \frac{\partial P}{\partial X} + \frac{1}{R_e}\left(\frac{\partial^2 U}{\partial X^2} + \frac{\partial^2 U}{\partial Y^2}\right)\Bigg\}, \quad (35)
\end{aligned}
$$

$\Longrightarrow$

$$
\begin{aligned}
p^n\mathscr{L}\{U(t)\} - p^{n-1}U(0) = \\
\left(p^n + \frac{n}{1-n}\right)\frac{1-n}{M(n)}\mathscr{L}\Bigg\{&-U\frac{\partial U}{\partial X} - V\frac{\partial U}{\partial Y} - R_f\left(U^2\frac{\partial^2 U}{\partial X^2}\right. \\
&\left. + V^2\frac{\partial^2 U}{\partial Y^2} + 2UV\frac{\partial^2 U}{\partial X \partial Y}\right) - \frac{\partial P}{\partial X} + \frac{1}{R_e}\left(\frac{\partial^2 U}{\partial X^2} + \frac{\partial^2 U}{\partial Y^2}\right)\Bigg\}, \quad (36)
\end{aligned}
$$

$\Longrightarrow$

$$
\begin{aligned}
p^n\mathscr{L}\{U(t)\} = p^{n-1}U(0) \\
+\left(\frac{(p^n + n + np^n)}{M(n)}\right)\mathscr{L}\Bigg\{&-U\frac{\partial U}{\partial X} \\
&- V\frac{\partial U}{\partial Y} - R_f\left(U^2\frac{\partial^2 U}{\partial X^2} + V^2\frac{\partial^2 U}{\partial Y^2}\right. \\
&\left. + 2UV\frac{\partial^2 U}{\partial X \partial Y}\right) - \frac{\partial P}{\partial X} + \frac{1}{R_e}\left(\frac{\partial^2 U}{\partial X^2} + \frac{\partial^2 U}{\partial Y^2}\right)\Bigg\}, \quad (37)
\end{aligned}
$$

This implies

$$
\begin{aligned}
\mathscr{L}\{U(t)\} = \frac{U(0)}{p} + \left(\frac{(1-n+np^{-n})}{M(n)}\right)\mathscr{L}\Bigg\{&-U\frac{\partial U}{\partial X} \\
&- V\frac{\partial U}{\partial Y} - R_f\left(U^2\frac{\partial^2 U}{\partial X^2} + V^2\frac{\partial^2 U}{\partial Y^2} + 2UV\frac{\partial^2 U}{\partial X \partial Y}\right) \\
&- \frac{\partial P}{\partial X} + \frac{1}{R_e}\left(\frac{\partial^2 U}{\partial X^2} + \frac{\partial^2 U}{\partial Y^2}\right)\Bigg\}, \quad (38)
\end{aligned}
$$

or

$$
\begin{aligned}
U(t) = U(0) + \mathscr{L}^{-1}\Bigg\{\left(\frac{(1-n+np^{-n})}{M(n)}\right)\mathscr{L}\Bigg\{&-U\frac{\partial U}{\partial X} \\
&- V\frac{\partial U}{\partial Y} - R_f\left(U^2\frac{\partial^2 U}{\partial X^2} + V^2\frac{\partial^2 U}{\partial Y^2} + 2UV\frac{\partial^2 U}{\partial X \partial Y}\right) \\
&- \frac{\partial P}{\partial X} + \frac{1}{R_e}\left(\frac{\partial^2 U}{\partial X^2} + \frac{\partial^2 U}{\partial Y^2}\right)\Bigg\}\Bigg\}. \quad (39)
\end{aligned}
$$

In an iterative setting,

$$
\begin{aligned}
U_{m+1}(t) = U(0) + \mathscr{L}^{-1}\Bigg\{\left(\frac{(1-n+np^{-n})}{M(n)}\right) \\
\mathscr{L}\Bigg\{-U_m\frac{\partial U_m}{\partial X} - V_m\frac{\partial U_m}{\partial Y} - R_f\left(U_m^2\frac{\partial^2 U_m}{\partial X^2} + V_m^2\frac{\partial^2 U_m}{\partial Y^2}\right. \\
\left. + 2U_mV_m\frac{\partial^2 U_m}{\partial X \partial Y}\right) - \frac{\partial P}{\partial X} + \frac{1}{R_e}\left(\frac{\partial^2 U_m}{\partial X^2} + \frac{\partial^2 U_m}{\partial Y^2}\right)\Bigg\}\Bigg\}. \quad (40)
\end{aligned}
$$

Now, to write the solution in Case 1, let $m = 0$ in (40), which implies

$$
\begin{aligned}
U_1(t) = U(0) + \mathscr{L}^{-1}\Bigg\{\left(\frac{(1-n+np^{-n})}{M(n)}\right)\mathscr{L}\Bigg\{&-U_0\frac{\partial U_0}{\partial X} \\
&- V_0\frac{\partial U_0}{\partial Y} - R_f\left(U_0^2\frac{\partial^2 U_0}{\partial X^2} + V_0^2\frac{\partial^2 U_0}{\partial Y^2} + 2U_0V_0\frac{\partial^2 U_0}{\partial X \partial Y}\right) \\
&- \frac{\partial P}{\partial X} + \frac{1}{R_e}\left(\frac{\partial^2 U_0}{\partial X^2} + \frac{\partial^2 U_0}{\partial Y^2}\right)\Bigg\}\Bigg\}. \quad (41)
\end{aligned}
$$

As $0 < n < 1$ therefore $M(n) = 1$, further assume $P$ to be constant, then and after utilizing the initial conditions in (41) we can write

$$U_1(t) = e^X + \left(\frac{e^X}{R_e} - e^{2X} - R_f e^{3X}\right)\left((1 - n + \frac{nt^n}{n!})\right). \quad (42)$$

Similarly, for $m = 1$ in (40) and after some simplifications, we get

$$\begin{aligned} U_2(t) = {} & e^X + \left(\frac{e^X}{R_e} - e^{2X} - e^{3X}\right)\left(1 - n + \frac{nt^n}{n!}\right) \\ & + \left(\frac{e^X}{R_e^2} - \frac{2e^{2X}}{R_e} - \frac{9R_f e^{3X}}{R_e} - \frac{e^{3X}}{R_e} + 4e^{4X} + 9R_f e^{5X}\right. \\ & \left. + 3e^{3X} + 4R_f e^{4X}\right)\left(1 - n + \frac{nt^n}{n!}\right)^2 - \left(\frac{e^{3X}}{R_e^2} + e^{5X} + R_f^2 e^{7X}\right. \\ & \left. - \frac{2e^{4X}}{R_e} + 2R_f e^{6X} - 2\frac{R_f}{R_e}e^{5X}\right)\left(1 - n + \frac{nt^n}{n!}\right)^3 \\ & - \left(\frac{e^{2X}}{R_e^2} - 3\frac{e^{3X}}{R_e} - 4\frac{R_f}{R_e}e^{4X} + 2e^{4X} + 5R_f e^{5X} + 3R_f^2 e^{6X}\right) \\ & \left(1 - n + \frac{nt^n}{n!}\right)^3 - \cdots. \end{aligned} \quad (43)$$

The solution of the system (15) is now obtained by $U(t) = U_0 + U_1 + U_2 + \cdots$ and thus reads

$$\begin{aligned} U(t) = {} & 2e^X + \left(\frac{2e^X}{R_e} - 2e^{2X} - (R_f + 1)e^{3X}\right)\left(1 - n + \frac{nt^n}{n!}\right) \\ & + \left(\frac{1}{R_e}\left(\frac{e^X}{R_e} - 2e^{2X} - 9R_f e^{3X}\right) - \frac{e^{3X}}{R_e} + 4e^{4X} + 9R_f e^{5X}\right. \\ & \left. - 3e^{3X} - 4R_f e^{4X}\right)\left(1 - n + \frac{nt^n}{n!}\right)^2 - \left(\frac{e^{3X}}{R_e^2} + e^{5X} + R_f^2 e^{7X}\right. \\ & \left. - \frac{2e^{4X}}{R_e} + 2R_f e^{6X} - 2\frac{R_f}{R_e}e^{5X}\right) \\ & \left(1 - n + \frac{nt^n}{n!}\right)^3 - \left(\frac{e^{2X}}{R_e^2} - 3\frac{e^{3X}}{R_e} - 4\frac{R_f}{R_e}e^{4X}\right. \\ & \left. + 2e^{4X} + 5R_f e^{5X} + 3R_f^2 e^{6X}\right)\left(1 - n + \frac{nt^n}{n!}\right)^3 - \left(\frac{e^{3X}}{R_e^3}\right. \\ & \left. + 9\frac{e^{5X}}{R_e} + 19\frac{R_f^2}{R_e}e^{7X} - 6\frac{e^{4X}}{R_e^2} + 28\frac{R_f}{R_e}e^{6X} - 22R_f^2 e^{8X} - 17R_f e^{7X}\right. \\ & \left. - \frac{11R_f e^{5X}}{R_e^2} - 4e^{6X} - 9R_f^3 e^{9X}\right)\left(1 - n + \frac{nt^n}{n!}\right)^4. \end{aligned} \quad (44)$$

Similarly, the solution in Case 2 is expressed as

$$\begin{aligned} U = {} & \left(\frac{6X + 2}{R_e} - X^2 - X^3\right)Y + \left(\frac{1}{R_e}(4R_f - 12X - 24R_f)\right. \\ & \left. - 4X^2 + 7X^3 R_e - X + 4\right)Y^2 + (13X^2 + 36R_f X - 12R_f/R_e)Y^3 \\ & + 8R_f/R_e Y^4 - 4/\mathrm{Re}^2 X, \end{aligned} \quad (45)$$

and

$$\begin{aligned} V = {} & \left(\frac{1}{R_e}\right)\left((4 - 4R_f)X^2 + R_f(8X - 12)^3 + (6X - 12X^2\right. \\ & \left. - 24R_f X^2 + 36R_f X^3)\right)Y - \left(4X^2 - 13X^3 - 8X^4\right)Y^4 + (7X^2 + 3X^3 \\ & - 32X^4)Y^3 + \left(4X^2 - 47X^3\right)Y^4 - 13X^2 Y^5. \end{aligned} \quad (46)$$

In Table 1, the effect of relaxation time and differential order is observed on the velocity profile at two selected points within the domain. It is observed that the velocity of the particles with the medium at the selected points is increased as the fractional order derivative is decreased. A reduction of 93.6% in the velocity is observed with a 10% increase in the fractional order of the derivative. Moreover, it is found that in the presence of relaxation time, the velocities of the particles are higher than in the case of without relaxation. The solution obtained is predicting a natural characteristic of increasing velocities by increasing the Reynolds number. Figure 2 plots the velocity profiles over the domain at varying time with the variation of the relaxation time factor. Reynold's number in these computations is kept constant at $Ra = 100$. The relaxation time factor is varied between $R_f = 0$ and $R_f = 0.2$. It can be seen from these computations that when $R_f = 0$ the maximum velocity of the particles is close

**Table 1**
Effect of Reynolds number, relaxation time and order on $U$-velocity

| $R_e$ | order | $U(0.5,1)$ | | $U(1,1)$ | |
|---|---|---|---|---|---|
| | | $R_f = 0$ | $R_f = 0.01$ | $R_f = 0$ | $R_f = 0.01$ |
| 100 | 0.9 | 4.607270585 | 4.623948405 | 11.24992525 | 11.41133054 |
| | 0.93 | 4.154751014 | 4.164093064 | 9.057627674 | 9.143094325 |
| | 0.95 | 3.878614048 | 3.884093905 | 7.794226682 | 7.841368265 |
| | 1.0 | 3.399961728 | 3.400544856 | 5.810255314 | 5.813794382 |
| 200 | 1.0 | 3.400134915 | 3.400718244 | 5.810553289 | 5.814093265 |
| 400 | 1.0 | 3.400221512 | 3.400804941 | 5.810702282 | 5.814242711 |
| 1000 | 1.0 | 3.400273471 | 3.400856960 | 5.810791679 | 5.814332381 |
| 2000 | 1.0 | 3.400290791 | 3.400874300 | 5.810821479 | 5.814362271 |

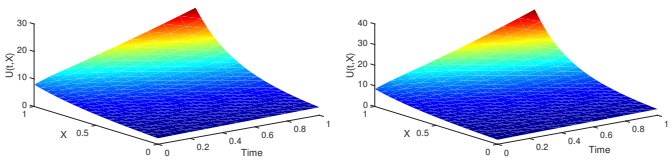


(a) $R_f = 0$ (b) $R_f = 0.1$

(c) $R_f = 0.15$ (d) $R_f = 0.2$

**Fig. 2.** $U$-velocity in Case 1 with $Ra = 100$ and varying $R_f$.

to 30. When $R_f = 0.1$ the velocity plateau gets increased and when $R_f$ is further increased to a value of 0.2 the velocity gets a further increase in its value. This indicates an increase in the velocity of the particles with an increasing relaxation time factor. Physically, the relaxation time factor represents the time required for the fluid particles to adjust to changes in the flow. A higher relaxation time suggests that the fluid has more time to respond to local stresses, increasing particle velocity. This can be interpreted as a slower adjustment to the shear forces, allowing the particles to attain higher velocities over time.

In Fig. 3 the $U$-velocities are plotted against time and the x-coordinate. The Reynolds number, similar to Fig. 2, $Ra$ is kept constant at 100, and the order of the fractional derivative is kept constant at $n = 0.05$. The fluid time relaxation, $R_f$ is varied from $0, 0.1, 0.3$ and $0.5$ and it is observed what are the corresponding peak $U$-velocities. It can be seen that when $R_f = 0$ the peak $U$-velocity is $U(X,t) = 7.5$, and as the value of $R_f$ is increased, velocities go from 8 to 9 to slightly over 10. The general trend is that with higher $R_f$ the velocities become higher too. Physically, the increase in velocity with higher relaxation time indicates that the fluid takes longer to respond to changes in the applied forces. A higher $R_f$ suggests a greater time for the particles to adjust to the local stresses, allowing the fluid to "relax" more before the velocity reaches its maximum. This behaviour is indicative of more pronounced viscoelastic effects, where the fluid has a greater ability to store and release energy, increasing the peak velocity as the relaxation time factor grows. In Fig. 4 the $U$-velocities are plotted concerning time and the $x$-coordinate. The Reynolds number $Ra$ is kept constant at 100 and the fluid time relaxation is kept constant at $R_f = 0.5$. Then we make a change in the order of the derivative to see what effect it has on the velocity. When the order of the derivative is $n = 1$, the peak $U$-velocity is at around $U(X,t) = 5$. As the order is increased to $n = 1.08$, the peak $U$-velocity goes to $U(X,t) = 6$, and at $n = 1.1$, the highest peak, at around $U(X,t) = 10$ is reached. The general trend that can be seen is that with the increase of the order of the derivative, the velocities also increase. For comparison of results, the reader is recommended to see [39]. Physically, this behaviour suggests that as the order of the fractional derivative increases, the system exhibits a greater degree of memory or history dependence in its flow behaviour. A higher-order derivative typically means that the fluid has a more pronounced nonlocal response to applied forces, where the velocity at any given time

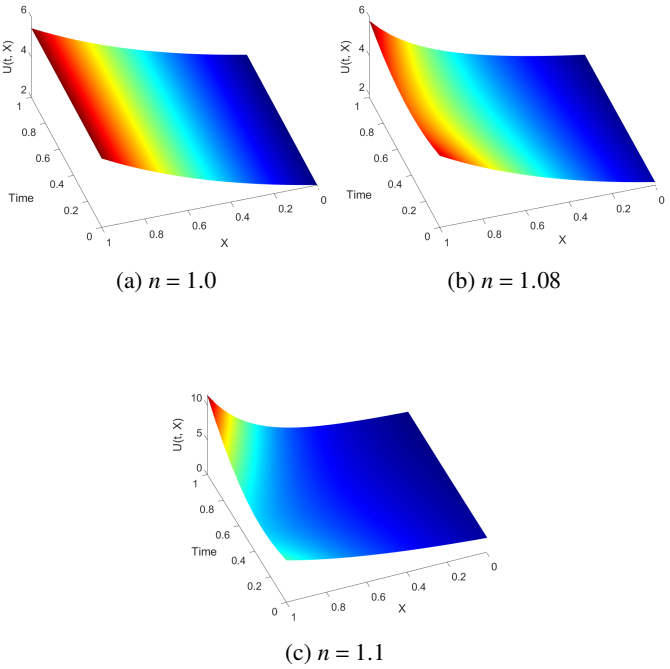


(a) $n = 1.0$ (b) $n = 1.08$

(c) $n = 1.1$

**Fig. 4.** $U$-velocity in Case 1, with $Ra = 100$, $R_f = 0.5$ and varying $n = 1.0.1.08$ and $1.1$

is influenced by a broader range of past states. This can lead to an increase in the peak velocities as the fluid exhibits enhanced responsiveness over time, reflecting more complex interactions between the particles and the flow. Figure 5 represents the effect of the fractional order of the derivative on the velocity profiles

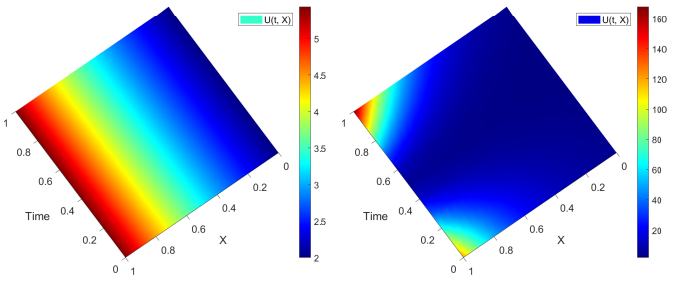


(a) $n = 1.0$ (b) $n = 1.5$

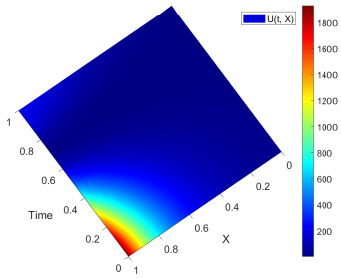


(c) $n = 2.0$

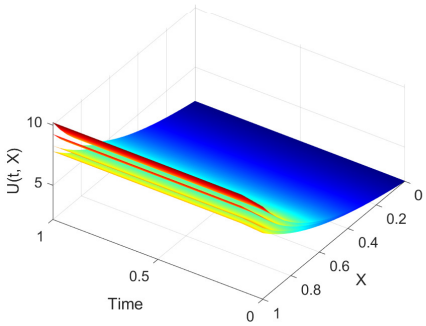


**Fig. 3.** $U$-velocity in Case 1 with $Ra = 100$, $n = 0.05$ and varying $R_f = 0, 0.1, 0.3, 0.5$

**Fig. 5.** Effect of order greater than one on the $U$-velocity in Case 1 with $Ra = 100$, and $R_f = 0.5$

within the domain of computation. Three different orders of the derivative are taken into observation for the velocity plots at a fixed Reynolds number. The relaxation time factor in these calculations is fixed at a value of 0.5. It is seen that fourth derivative of order one the velocity is linearly distributed over the domain in $x$-direction in time, whereas a nonlinear distribution is exhibited while the fractional order of the differentiation is increased. Moreover, this nonlinear distribution becomes highly nonsymmetric over the domain and over time when the fractional order is taken to be two. As in Case 1, the second initial for $V$ is the same as the one for $U$, it results in the same final results for the V velocities as were obtained for the $U$ velocities.

In Fig. 6, the $U$-velocity is plotted from Case 2 against time and the x-coordinate. The Reynolds number is kept constant at 100, and the order of the fractional derivative is fixed at 0.7. The y-coordinate is also fixed at 0.15. The fluid time relaxation is varied to observe the effect it may have on the magnitude of velocity, and it can be observed that when $R_f = 1$, the $U$-velocity crosses 6. A slight increase can be observed as $R_f$ is changed to 1.3 and 1.7. As soon as $R_f$ becomes 2, our peak velocity touches 10. This concludes that as the fluid time relaxation is increased, the velocity increases.

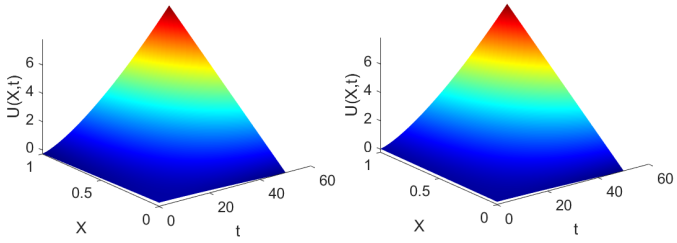


(a) $R_f = 1$ (b) $R_f = 1.7$

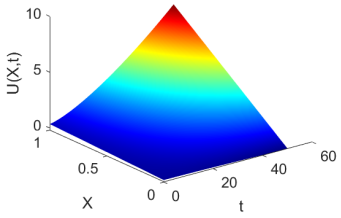


(c) $R_f = 2$

**Fig. 6.** $U$-velocity in Case 2, with $Ra = 100$, $n = 0.7$, and $y = 0.15$

In Fig. 7, the Reynolds number is kept constant at 100, the fluid relaxation is fixed at 1.5, and the y-coordinate is set to 0.05. The order of the derivative is varied to observe its effect on the magnitudes of velocity. Graphs are plotted for the $U$-velocities against the x-coordinate and time. It can be seen that velocity is at its lowest when the order of the derivative is lowest at 0.5, hitting a peak velocity at around 3. As the order is increased to 0.6, the peak velocity surpasses 5. When it is further increased to 0.8, the velocity crosses 20, and finally, it hits a new high, surpassing 40, when the order is changed to 0.9. This concludes that as the order increases, so do the $U$-velocities. Physically, this behaviour can be explained by the increasing effect of the fractional derivative on the fluid flow. As the order of the derivative increases, the fluid memory effect becomes more pronounced, resulting in a higher sensitivity to past states and a greater response to the forces acting on the fluid. This leads to an increase in the peak velocities. The sharp rise in velocity as the order increases, especially between 0.8 and 0.9, suggests that the fluid exhibits more complex, nonlocal interactions at higher derivative orders.

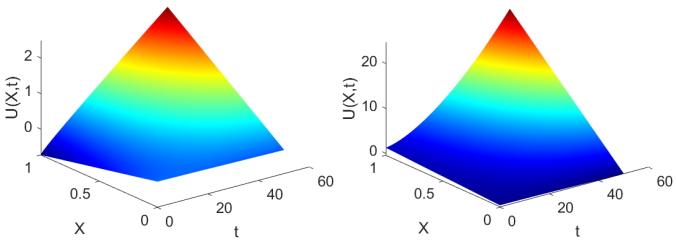


(a) $n = 0.5$ (b) $n = 0.8$

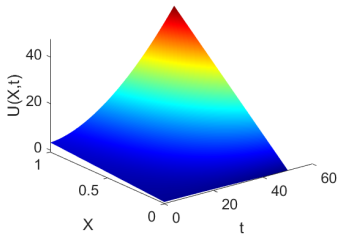


(c) $n = 0.9$

**Fig. 7.** $U$-velocity in Case 2, with $Ra = 100$, $R_f = 1.5$, and $y = 0.05$

In Fig. 8, the velocity $V(Y,t)$ is shown for Case 2, where the Reynolds number is fixed at $Ra = 100$, the fluid relaxation time is set to $R_f = 1.5$, and the $x$-coordinate is held constant at $x = 0.05$. The plot captures the variation of the velocity concerning the y-coordinate and time, providing insight into how the velocity

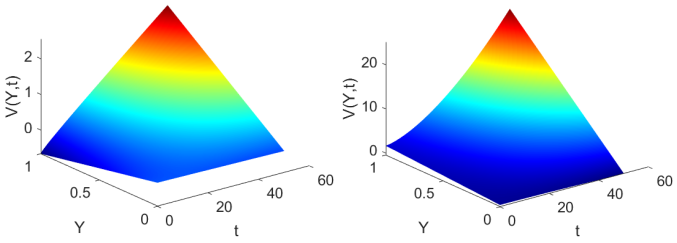


(a) $n = 0.5$ (b) $n = 0.8$

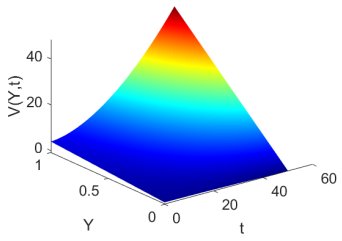


(c) $n = 0.9$

**Fig. 8.** $V$-velocity in Case 2, with $Ra = 100$, $R_f = 1.5$, and $x = 0.05$

evolves under these conditions when the order of the fractional derivative is increased from $n = 0.5$ to $n = 0.8$, and finally to $n = 0.9$. The results reveal the dynamic behaviour of the system, highlighting the influence of the specified parameters on the velocity profile. We can observe that when the order is minimal, the V-velocity is peaking at 2. When the order is 0.8, velocity peaks around 20. And finally, when the order is 0.9, the velocity is peaking around 40.

This approach offers several advantages over traditional methods. By incorporating the Atangana-Baleanu fractional derivative, it captures memory effects and nonlocal behaviour, which are often present in complex physical systems but overlooked in standard models. The use of Laplace transforms simplifies solving partial differential equations, converting them into algebraic equations in the frequency domain, which are easier to handle. The iterative solution approach allows for a more accurate and refined solution by progressively improving the approximation, especially for systems with nonlinearities or complex boundary conditions. In general, this method provides a more flexible and accurate framework for solving PDE systems in cases where classical approaches may fail.

## 6. CONCLUSIONS

In this work, the analytical solution of a viscoelastic fractional-time relaxation model is obtained by combining the Laplacian approach with a distinctive method based on the Atangana-Baleanu fractional calculus. The upper convected Maxwell constitutive relaxation equation serves as the foundation for the fractional time relaxation model. The results on the existence and uniqueness of the solution are established. For the underlying viscoelastic model of physical-time relaxation, analytical representations of the solutions are found. The complex behaviour of a two-dimensional viscoelastic fluid is examined using two test models specified with initial conditions. Examines and explains how important parameters, such as Reynolds number, relaxation time, and order of the fractional derivative, affect the properties of fluid flow in the dynamics considered. The results show that as the relaxation time factor ($R_f$) increases, the velocity of the particles also increases. Furthermore, a higher order of the derivative leads to an overall increase in velocities, demonstrating the significant effect of both parameters on flow dynamics. Moreover, it is observed that as the fractional order of the differentiation increases, a nonlinear distribution is observed, while for a derivative of order one, the velocity is linearly distributed over the domain in the $x$-direction in time. Furthermore, when the fractional order is assumed to be two, this nonlinear distribution becomes extremely nonsymmetric over the domain and over time.

This work demonstrates the powerful capability of fractional calculus in modelling complex viscoelastic systems, offering deeper insight into the dynamic behaviour of fluid flows that classical methods may overlook. The incorporation of fractional-time relaxation and Laplace transforms provides a more robust framework for understanding the interplay between physical parameters like Reynolds number and relaxation time. Moving forward, future research could explore the extension of this model to three-dimensional systems or more complex geometries, as well as the application of other fractional operators to capture different types of memory effects. Additionally, experimental validation of the model could be pursued to further refine the theoretical predictions and improve its applicability in real-world scenarios, particularly in industrial and environmental fluid dynamics.

## APPENDIX

To nondimensionalize the equations governing the two-dimensional unsteady incompressible viscoelastic flow, we introduce the following dimensionless variables.

$$\begin{aligned} U &= \frac{u}{u_0}, \quad V = \frac{v}{u_0}, \quad T = \frac{tL}{u_0}, \\ X &= \frac{x}{L}, \quad Y = \frac{y}{L}, \quad P = \frac{p}{\rho u_0^2}, \end{aligned} \tag{47}$$

where $u_0$ is the characteristic velocity, $L$ is the characteristic length, and $\rho$ is the density.

### Continuity equation

The continuity equation in dimensional form is given as

$$\frac{\partial u}{\partial x} + \frac{\partial v}{\partial y} = 0. \tag{48}$$

To nondimensionalize this equation, we replace $u$, $v$, $x$ and $y$ by their dimensionless counterparts such that

$$\frac{\partial u}{\partial x} = \frac{u_0}{L}\frac{\partial U}{\partial X},$$

and

$$\frac{\partial v}{\partial y} = \frac{u_0}{L}\frac{\partial V}{\partial Y}.$$

Thus, the nondimensionalized continuity equation becomes

$$\frac{\partial U}{\partial X} + \frac{\partial V}{\partial Y} = 0. \tag{49}$$

### X-momentum equation

The dimensional form of the $x$-momentum equation is given as

$$\begin{aligned} D_t^{\alpha}(u) + u\frac{\partial u}{\partial x} + v\frac{\partial u}{\partial y} + \lambda\left(u^2\frac{\partial^2 u}{\partial x^2} + v^2\frac{\partial^2 u}{\partial y^2} + 2uv\frac{\partial^2 u}{\partial x \partial y}\right) \\ = -\frac{1}{\rho}\frac{\partial p}{\partial x} + \eta\left(\frac{\partial^2 u}{\partial x^2} + \frac{\partial^2 u}{\partial y^2}\right). \end{aligned} \tag{50}$$

The following dimensionless variables are utilized.

$$u = u_0 U, \quad v = u_0 V, \quad x = LX, \quad y = LY, \quad t = \frac{Tu_0}{L}.$$

The time derivative is nondimensionalized as follows.

$$D_t^{\alpha}(u) = \frac{u_0}{L}\frac{d^{\alpha}}{dT^{\alpha}}U.$$

The spatial derivatives become

$$\frac{\partial u}{\partial x} = \frac{u_0}{L}\frac{\partial U}{\partial X}, \quad \frac{\partial u}{\partial y} = \frac{u_0}{L}\frac{\partial U}{\partial Y}, \quad \text{and} \quad \frac{\partial^2 u}{\partial x^2} = \frac{u_0}{L^2}\frac{\partial^2 U}{\partial X^2}.$$

Similarly, we can express pressure $p$ and its gradient as

$$\frac{\partial p}{\partial x} = \frac{\rho u_0^2}{L}\frac{\partial P}{\partial X}.$$

Substituting all the above terms into the $x$-momentum equation, we get the following nondimensionalized form.

$$\begin{aligned}\frac{u_0}{L}\frac{d^\alpha}{dT^\alpha}U + u_0\left(u_0 U\frac{\partial U}{\partial X} + u_0 V\frac{\partial U}{\partial Y}\right) \\ + \lambda u_0^2\left(U^2\frac{\partial^2 U}{\partial X^2} + V^2\frac{\partial^2 U}{\partial Y^2} + 2UV\frac{\partial^2 U}{\partial X \partial Y}\right) \\ = -\frac{u_0}{\rho L}\frac{\rho u_0^2}{L}\frac{\partial P}{\partial X} + \eta\frac{u_0}{L^2}\left(\frac{\partial^2 U}{\partial X^2} + \frac{\partial^2 U}{\partial Y^2}\right). \end{aligned} \tag{51}$$

Simplifying the nondimensionalized terms, the equation becomes

$$\begin{aligned}\frac{d^\alpha}{dT^\alpha}U + U\frac{\partial U}{\partial X} + V\frac{\partial U}{\partial Y} + \lambda\left(U^2\frac{\partial^2 U}{\partial X^2} + V^2\frac{\partial^2 U}{\partial Y^2} + 2UV\frac{\partial^2 U}{\partial X \partial Y}\right) \\ = -\frac{\partial P}{\partial X} + \frac{1}{Re}\left(\frac{\partial^2 U}{\partial X^2} + \frac{\partial^2 U}{\partial Y^2}\right). \end{aligned} \tag{52}$$

### Y-momentum equation

The nondimensionalization process for the $y$-momentum equation follows similarly. Starting with the dimensional form

$$\begin{aligned}D_t^\alpha(v) + u\frac{\partial v}{\partial x} + v\frac{\partial v}{\partial y} + \lambda\left(u^2\frac{\partial^2 v}{\partial x^2} + v^2\frac{\partial^2 v}{\partial y^2} + 2uv\frac{\partial^2 v}{\partial x \partial y}\right) \\ = -\frac{1}{\rho}\frac{\partial p}{\partial y} + \eta\left(\frac{\partial^2 v}{\partial x^2} + \frac{\partial^2 v}{\partial y^2}\right). \end{aligned} \tag{53}$$

Following the same procedure as above, we substitute the dimensionless variables and obtain the nondimensionalized $y$-momentum equation as

$$\begin{aligned}\frac{d^\alpha}{dT^\alpha}V + U\frac{\partial V}{\partial X} + V\frac{\partial V}{\partial Y} + \lambda\left(U^2\frac{\partial^2 V}{\partial X^2} + V^2\frac{\partial^2 V}{\partial Y^2} + 2UV\frac{\partial^2 V}{\partial X \partial Y}\right) \\ = -\frac{\partial P}{\partial Y} + \frac{1}{\mathrm{Re}}\left(\frac{\partial^2 V}{\partial X^2} + \frac{\partial^2 V}{\partial Y^2}\right). \end{aligned} \tag{54}$$

## REFERENCES

[1] Z. Mengnan, Y. Erjie, J. Zeng, J. Ji, F. Tian, and L. Li, "Numerical study on oblique stretching of viscoelastic polymer film," *J. Non-Newton. Fluid Mech.*, vol. 295, p. 104597, 2021, doi: 10.1016/j.jnnfm.2021.104597.

[2] D. Tang, F. Marchesini, L. Cardon, and D. D'hooge, "Three-dimensional flow simulations for polymer extrudate swell out of slit dies from low to high aspect ratios," *Phys. Fluids*, vol. 31, p. 093103, 2019, doi: 10.1063/1.5116850.

[3] C. Czibula, T. Seidlhofer, C. Ganser, U. Hirn, and C. Teichert, "Longitudinal and transverse low frequency viscoelastic characterization of wood pulp fibers at different relative humidity," *Materialia*, vol. 16, p. 101094, 2021, doi: 10.1016/j.mtla.2021.101094.

[4] S. Stieger *et al.*, "On the Influence of Viscoelastic Modeling in Fluid Flow Simulations of Gum Acrylonitrile Butadiene Rubber," *Polymers*, 2021, doi: 10.3390/polym13142323.

[5] M. S. Kassim and S. Sarow, "Flows of Viscous Fluids in Food Processing Industries: A review," *IOP Conference Series: Materials Science and Engineering*, vol. 870, p. 012032, 2020, doi: 10.1088/1757-899X/870/1/012032.

[6] Z. Chen and D. Ceballos-Francisco, "The alleviation of skin wound-induced intestinal barrier dysfunction via modulation of TLR signalling using arginine in gilthead seabream (Sparus aurata L)," *Fish Shellfish Immunol.*, vol. 870107, pp. 519–528, 2020.

[7] M. Pelton, D. Chakraborty, E. Malachosky, G.-S. Philippe, and J. Sader, "Viscoelastic flows in simple liquids generated by vibrating nanostructures," *Phys. Rev. Lett.*, vol. 111, p. 244502, 2013, doi: 10.1103/PhysRevLett.111.244502.

[8] B. Qin, "Flow behavior and instabilities in viscoelastic fluids: physical and biological systems," *Publicly Accessible Penn Dissertations, University of Pennsylvania*, vol. 3174, 2018.

[9] C. Yuan, H.N. Zhang, Y. Li, X.-B. Li, J. Wu, and F.-C. Li, "Nonlinear effects of viscoelastic fluid flows and applications in microfluidics: A review," *Proc. Inst. Mech. Eng. Part C-J. Eng. Mech. Eng. Sci.*, vol. 234, p. 095440622092286, 2020, doi: 10.1177/0954406220922863.

[10] E.L.L. Zhu and L. Brandt, "Self-propulsion in viscoelastic fluids: pushers vs. pullers," *Phys. Fluids*, vol. 24, no. 5, p. 051902, 2012.

[11] B. Sebastian and P. Dittrich, "Microfluidics to mimic blood flow in health and disease," *Annu. Rev. Fluid Mech.*, vol. 50, pp. 483–504, 2018, doi: 10.1146/annurev-fluid-010816-060246.

[12] S. Haward, K. Toda-Peters, and A. Shen, "Steady viscoelastic flow around high-aspect-ratio, low-blockage-ratio microfluidic cylinders," *J. Non-Newton. Fluid Mech.*, vol. 254, pp. 23–35, 2018, doi: 10.1016/j.jnnfm.2018.02.009.

[13] P. Liu *et al.*, "Length-based separation of bacillus subtilis bacterial populations by viscoelastic microfluidics," *Microsyst. Nanoeng.*, vol. 8, p. 7, 2021, doi: 10.1038/s41378-021-00333-3.

[14] M. Alves, P. Oliveira, and F. Pinho, "Numerical methods for viscoelastic fluid flows," *Annu. Rev. Fluid Mech.*, vol. 53, pp. 1–33, 2020, doi: 10.1146/annurev-fluid-010719-060107.

[15] M. Khan, M. Memon, and E. Bonyah, "Investigation of relaxation time on viscoelastic two-dimensional flow characteristics using freefem++," *J. Math.*, vol. 2022, pp. 1–15, 2022, doi: 10.1155/2022/4977793.

[16] D. Baleanu, A. Jajarmi, H. Mohammadi, and S. Rezapour, "A new study on the mathematical modelling of human liver with caputo-fabrizio fractional derivative," *Chaos Solitons Fractals*, vol. 134, p. 109705, 2020, doi: 10.1016/j.chaos.2020.109705.

[17] O. Defterli, D. Baleanu, A. Jajarmi, S.S. Sajjadi, N. Alshaikh, and J.H. Asad, "Fractional treatment: an accelerated mass-spring system," *Rom. Rep. Phys.*, vol. 74, p. 122, 2022.

[18] A. Khan, T. Abdeljawad, and H. Khan, "A numerical scheme for the generalized abc fractional derivative based on lagrange interpolation polynomial," *Fractals*, vol. 30, p. 2240180, 2022, doi: 10.1142/S0218348X22401806.

[19] S. Hussain, E.N. Madi, H. Khan, and M. Abdo, "A numerical and analytical study of a stochastic epidemic sir model in the light of white noise," *Adv. Math. Phys.*, vol. 2022, pp. 1–9, 2022, doi: 10.1155/2022/1638571.

[20] C. Xu, Z. Liu, Y. Pang, and A. Akgül, "Stochastic analysis of a covid-19 model with effects of vaccination and different transition rates: Real data approach," *Chaos Solitons Fractals*, vol. 170, p. 113395, 2023, doi: 10.1016/j.chaos.2023.113395.

[21] C. Xu, M. Farman, A. Hasan, A. Akgül, M. Zakarya, W. Albalani, and C. Park, "Lyapunov stability and wave analysis of covid-19 omicron variant of real data with fractional operator," *Alex. Eng. J.*, vol. 61, pp. 11 787–11 802, 2022, doi: 10.1016/j.aej.2022.05.025.

[22] S. Yao, M. Farman, A. Akgül, K. Nisar, M. Amin, M.U. Saleem, and M. Inc, "Simulations and analysis of covid-19 as a fractional model with different kernels," *Fractals*, vol. 31, no. 4, p. 2340051, 2023, doi: 10.1142/S0218348X23400510.

[23] M. Amin, M. Farman, A. Akgül, and R. Alqahtani, "Effect of vaccination to control covid-19 with fractal fractional operator," *Alex. Eng. J.*, vol. 61, pp. 3551–3557, 2021, doi: 10.1016/j.aej.2021.09.006.

[24] M. Farman, M. Amin, A. Akgül, A. Ahmad, M. Riaz, and S. Ahmad, "Fractal fractional operator for covid-19 (omicron) variant outbreak with analysis and modeling," *Results Phys.*, vol. 39, p. 105630, 2022, doi: 10.1016/j.rinp.2022.105630.

[25] E. Uçar and N. Ozdemir, "New fractional cancer mathematical model via il-10 cytokine and anti-pd-l1 inhibitor," *Fractal Fract.*, vol. 7, p. 151, 2023, doi: 10.3390/fractalfract7020151.

[26] E. Uçar, S. Uçar, F. Evirgen, and N. Özdemir, "A fractional saidr model in the frame of atangana–baleanu derivative," *Fractal Fract.*, vol. 5, no. 2, p. 32, 2021, doi: 10.3390/fractalfract5020032.

[27] N. Ozdemir and E. Uçar, "Investigating of an immune system-cancer mathematical model with mittag-leffler kernel," *AIMS Math.*, vol. 5, pp. 1519–1531, 2020, doi: 10.3934/math.2020104.

[28] F. Evirgen, E. Uçar, S. Uçar, and N. Ozdemir, "Modelling influenza A disease dynamics under Caputo-Fabrizio fractional derivative with distinct contact rates," *Math. Model. Numer. Simul. Appl.*, vol. 3, pp. 58–73, 2023, doi: 10.53391/mmnsa.1274004.

[29] F. Evirgen, E. Uçar, N. Ozdemir, E. Altun, and T. Abdeljawad, "The impact of non-singular memory on the mathematical model of Hepatitis C virus," *Fractals*, vol. 31, no. 04, p. 2340065, 2023, doi: 10.1142/S0218348X23400650.

[30] M. Syam and M. Al-Refai, "Fractional differential equations with atangana–baleanu fractional derivative: Analysis and applications," *Chaos Solitons Fractals*, vol. 2, p. 100013, 2019, doi: 10.1016/j.csfx.2019.100013.

[31] A.M. Alqahtani and A. Shukla, "Computational analysis of multi-layered navier–stokes system by atangana–baleanu derivative," *Appl. Math. Sci. Eng.*, vol. 32, no. 1, p. 2290723, 2024, doi: 10.1080/27690911.2023.2290723.

[32] L. Abdelhaq, M. Syam, and M. Syam, "An efficient numerical method for two-dimensional fractional integro-differential equations with modified atangana-baleanu fractional derivative using operational matrix approach," *Partial Differ. Equ. Appl. Math.*, vol. 11, p. 100824, 2024, doi: 10.1016/j.padiff.2024.100824.

[33] A. Ghafoor, M. Fiaz, K. Shah, and T. Abdeljawad, "Analysis of nonlinear burgers equation with time fractional atangana-baleanu-caputo derivative," *Heliyon*, vol. 10, no. 13, p. e33842, 2024.

[34] A. Fathy, M. Semary, and H. Hassan, "An approximate solution of fractional order riccati equations based on controlled picard's method with atangana–baleanu fractional derivative," *Alex. Eng. J.*, vol. 61, 2021, doi: 10.1016/j.aej.2021.09.009.

[35] W. Shatanawi *et al.*, "A fractional dynamics of tuberculosis (tb) model in the frame of generalized atangana–baleanu derivative," *Results Phys.*, vol. 29, p. 104739, 2021, doi: 10.1016/j.rinp.2021.104739.

[36] S. Altoum, "An efficient numerical approach for solving systems of fractional problems and their applications in science," *Mathematics*, vol. 11, p. 3132, 2023, doi: 10.3390/math11143132.

[37] E. Bas and R. Ozarslan, "Real world applications of fractional models by atangana–baleanu fractional derivative," *Chaos Solitons Fractals*, vol. 116, pp. 121–125, 2018, doi: 10.1016/j.chaos.2018.09.019.

[38] D. Baleanu and B. Shiri, "Numerical methods for solving systems of atangana-baleanu fractional differential equations," in *Applications of Fractional Calculus to Modeling in Dynamics and Chaos*. Chapman and Hall/CRC, 2022, pp. 353–378.

[39] M. Yavuz, N. Sene, and M. Yıldız, "Analysis of the influences of parameters in the fractional second-grade fluid dynamics," *Mathematics*, vol. 10, no. 7, p. 1125, 2022, doi: 10.3390/math10071125.